Electron temperatures in the Galactic H II regions W43 and M17

Ravi Subrahmanyan[1,3] and W. M. Goss[2]

[1]*Raman Research Institute, Sadashivanagar, Bangalore 560 080, India*
[2]*National Radio Astronomy Observatory, PO Box 0, Socorro, NM 87801, USA*
[3]*Australia Telescope National Facilitiy, CSIRO, PO Box 76, Epping, NSW 2121, Australia*

ABSTRACT

We present 1.2-arcmin resolution images of the Galactic H II regions W43 and M17 made with the Very Large Array (VLA) at a frequency of 330 MHz; these are the highest resolution images to date of the large-scale structures of these complexes at any frequency. The electron temperature towards the component of W43 that has the highest emission measure, $G30.8 - 0.0$, is 5410 ± 300 K. The electron temperatures towards the components of M17, $G15.0 - 0.7$ and $G15.1 - 0.7$, are 7600^{+700}_{-210} and 8000^{+450}_{-220} K respectively. These estimates are consistent with previous estimates based on radio recombination line and continuum observations of these H II regions.

Key words: H II regions – ISM: individual: M17 – ISM: individual: W43 – radio continuum: ISM.

1 INTRODUCTION

The physics of the radiative transfer in thermal gaseous nebulae is described by Osterbrock (1989). Bright emission nebulae that have a high emission measure (EM), exceeding 10^6 pc cm^{-6} towards their centres, are expected to have optical depths $\tau > 1$ over their central regions at radio frequencies below 1 GHz. Consequently, the observed brightness temperature towards their opaque centres is a direct measurement of the electron temperature in the thermal gas. Metre-wavelength radio-continuum imaging of these H II regions is, therefore, a method of deriving the electron temperatures T_e in their thermal gas.

Low-frequency imaging of H II regions for the purpose of determining the electron temperatures has been attempted in the past (Shaver 1969; Copetti & Schmidt 1991), but the errors in the derived temperatures have been large because of the limited angular resolutions ($\gtrsim 3$ arcmin) then available. We have used the Very Large Array (VLA; Napier, Thompson & Ekers 1983) at 330 MHz to image a sample of bright, extended H II regions – M42, NGC 2024, W51, M17 and W43 – with 1.2-arcmin resolution: all these regions have maximum angular extents of about half a degree and may be imaged within the VLA 330-MHz primary beams; their opaque cores (at 330 MHz) are expected to exceed 1 arcmin. The estimates of T_e of 7865 ± 360 K towards M42, 8400 ± 1000 K towards NGC 2024 and 7800 ± 300 K towards W51 are published elsewhere (Subrahmanyan 1992a, b; Subrahmanyan & Goss 1995); observations of W43 and M17 are presented here.

2 OBSERVATIONS

The H II regions W43 and M17 were each observed for 2 h around transit in the D array configuration of the VLA in September 1992 and in the C array configuration during July 1993. The radio continuum observations were made using a pair of 3.125-MHz wide bands centred at 327.5 and 333.0 MHz. The absolute flux density scale was established by observations of 3C 48, the flux density of which has been adopted to be 44.70 and 44.28 Jy respectively at 327.5 and 333.0 MHz based on the BGPW scale (Baars et al. 1977). Observations of 3C 48 with the VLA have shown that this flux density value is accurate to within 2 per cent (Perley & Crane 1986). The visibility phases and temporal gain changes were calibrated by half-hourly observations of the unresolved calibrator source 3C 380. The visibility data were also self-calibrated in amplitude and phase using the standard NRAO Astronomical Image Processing Software (AIPS) prior to imaging using the 3D imaging routines in Software Development Environment (SDE) implemented by T. J. Cornwell. The images were corrected for the attenuation because of the telescope primary beam.

3 330-MHz IMAGE OF W43

The 330-MHz image of the W43 region, made with a beam of 71.9×68.8 arcsec^2 full width half maximum (FWHM) at a position angle of $26^\circ.1$, is shown in Fig. 1. The bright nebulosity at the centre of the image is $G30.8 - 0.0$ with a peak flux density of 2.02 Jy beam^{-1}. The distances to the
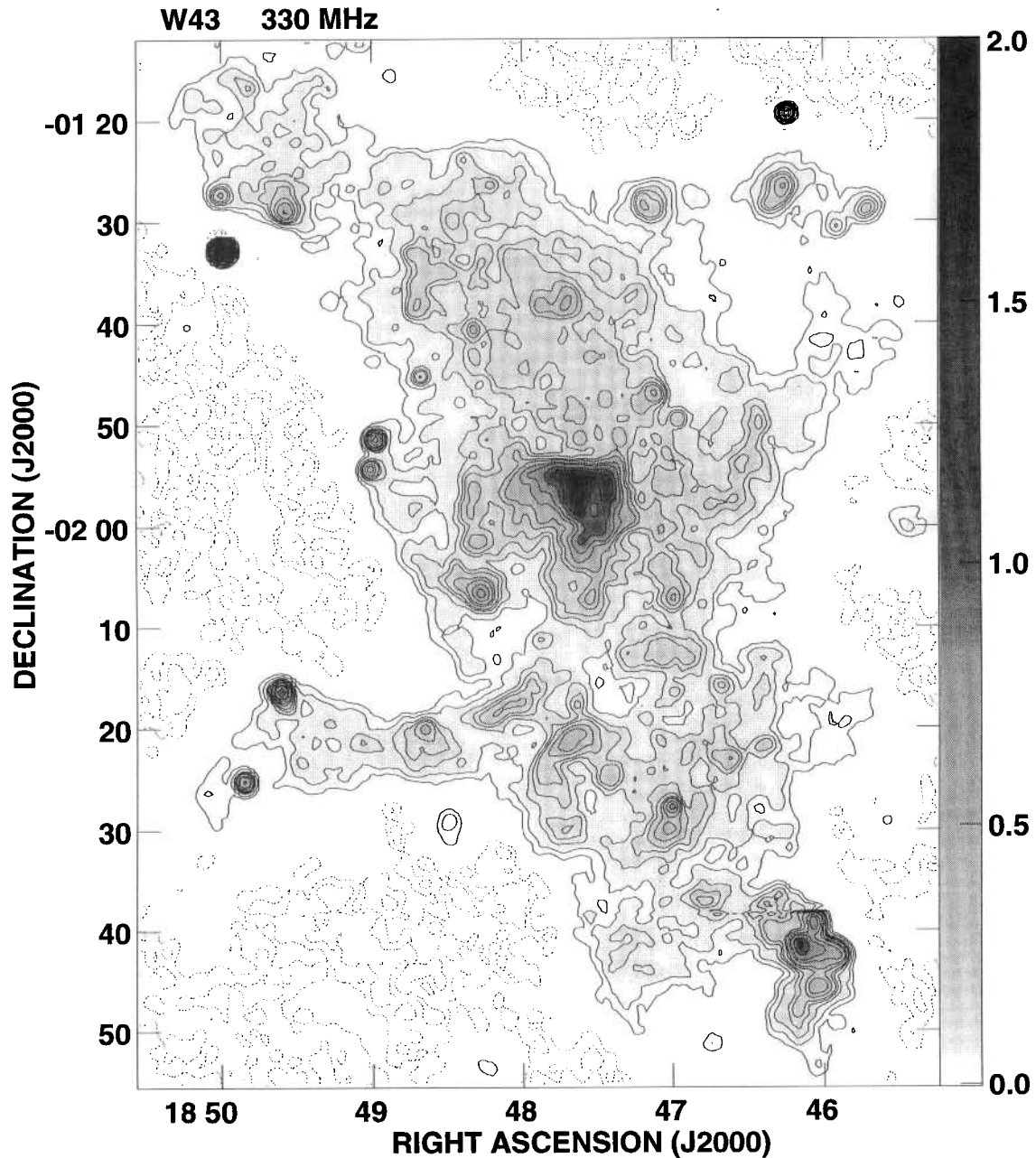
Figure 1. 330-MHz image of W43 made with a beam of 71.9×68.8 arcsec^2 at a position angle (PA) of 26°.1. Contours are at 10 mJy beam$^{-1} \times (-8, -4, -2, 2, 4, 8, 12, 16, 24, 32, 48, 64, 96, 128, 192, 256, 384, 512, 768)$. Grey-scales are shown in the range 0–2 Jy beam^{-1}.

thermal sources in W43 have been estimated to be between 7 and 8.5 kpc based on the detection of H134α recombination lines (Gardner & Thomasson 1975) from several components of the nebula. For an assumed distance of 7.8 kpc for this source complex, 10 arcmin angular distance corresponds to 23 pc.

Previous images of the large-scale structure of W43 are the 2.6-arcmin resolution image made at 4.875 GHz by Altenhoff et al. (1978), the 4-arcmin image made by Goss & Shaver (1970) at 5 GHz and the 2.8-arcmin image made by Shaver & Goss (1970) at 408 MHz. Higher resolution images of G30.8 − 0.0 have been produced with the VLA: a 12.5-arcsec resolution image was made by Liszt, Braun &

Greisen (1993) at 1.4 GHz and an 8-arcsec image was made by Lester et al. (1985) at 5 GHz.

Because our image of W43 has been made with the VLA, which is a Fourier-synthesis telescope that uses only visibility measurements made between spatially-separated antennas to synthesise images, the uniform emission present in the sky will be missing in the synthetic image. We assume that the uniform missing background in the 330-MHz interferometric image is entirely the result of the Galactic synchrotron emission, and has a spectral index $\alpha = -0.6$ (we define the spectral index as $S_\nu \sim \nu^\alpha$). The Galactic-plane image made by Large, Mathewson & Haslam (1961), with the zero level corrected to be 100 K,

suggests that the Galactic background brightness temperature T_{bg} at 408 MHz is 315 ± 43 K in the vicinity of W43. The all-sky survey of Haslam et al. (1982) indicates a $T_{bg} = 330 \pm 50$ K at 408 MHz. A higher frequency survey of the Galactic plane at 4.875 GHz (Altenhoff et al. 1978) has a background brightness of 0.5 ± 0.1 K near W43. Adopting a spectral index $\beta = -2.6$ for the background temperature ($T_{bg} \sim v^\beta$), we infer corresponding estimates for T_{bg} at 330 MHz; their weighted mean is 560 ± 50 K. This missing uniform background corresponds to a missing flux density of 0.25 ± 0.02 Jy beam^{-1} in Fig. 1.

Because W43 has an angular extent exceeding 30 arcmin on the sky, the VLA 330-MHz image of the object may not have reproduced the largest-scale structure in the source. We compared the images of W43 made with single-dish telescopes at 4.875 GHz (Altenhoff et al. 1978) and at 5 GHz (Goss & Shaver 1970) with the 330-MHz image smoothed to their resolutions. Assuming a uniform Galactic background of $T_{bg} = 0.5 \pm 0.1$ K at 5 GHz, and assuming further that the emission towards the outer parts of W43 are optically thin at 330 MHz, we find no conclusive evidence for missing flux density in the 330-MHz image: the missing flux density in the 330-MHz image in Fig. 1 owing to extended thermal emission associated with W43 is at most 0.08 Jy beam^{-1}.

We have smoothed the 330-MHz image of W43 to a resolution of 2.6 arcmin, corresponding to the resolution of the 4.875-GHz image in Altenhoff et al. (1978), and compared the peak intensities at the two frequencies towards the various components. The source names, sky coordinates and peak flux densities at the two frequencies are listed in Table 1. The peak flux densities listed at 5 GHz (S_2) have been obtained after subtracting 0.3 Jy beam^{-1}, corresponding to the background emission; the values listed at 330 MHz (S_1) are the peak flux densities in the smoothed 330-MHz interferometric image. We make the assumption that the individual H II regions in W43 are isothermal. We also assume that W43 is optically thin ($\tau_2 \ll 1$) over the entire nebula at the higher frequency, $v_2 = 5$ GHz. Consequently, the observed brightness temperatures of the H II regions at v_2, equivalent to the flux densities S_2 listed in column 5 of the table, are expected to be

$$T_2 \approx \tau_2 T_e, \tag{1}$$

where T_e are the electron temperatures in the H II regions. Since the optical depth towards isothermal H II regions may be approximated by

$$\tau \approx 8.235 \times 10^{-2} T_e^{-1.35} v^{-2.1} \text{EM}, \tag{2}$$

where the EM is in pc cm^{-6} and the frequency v is in GHz, the optical depth τ_2 at v_2 may be written in terms of the optical depth τ_1 at v_1 as $\tau_2 = \tau_1(v_2/v_1)^{-2.1}$. Consequently,

$$T_2 \approx \tau_1 T_e (v_2/v_1)^{-2.1}. \tag{3}$$

The brightness temperatures equivalent to the peak flux densities S_1 at $v_1 = 330$ MHz, which are listed in column 4 of the table, are expected to correspond to

$$T_1 = T_{bg} e^{-\tau_1} + T_e(1 - e^{-\tau_1}) - T_{bg} \tag{4}$$

for the H II regions because the 330-MHz image has a constant brightness of value T_{bg} missing throughout. Eliminating T_e and expressing the brightness temperatures in terms of flux densities, we find

$$S_1 = \left[\frac{S_2}{\tau_1}\left(\frac{v_2}{v_1}\right)^{0.1} - S_{bg}\right](1 - e^{-\tau_1}). \tag{5}$$

S_{bg}, of value 1.21 Jy beam^{-1}, is the missing flux density expected in the 2.6-arcmin beam arising from the missing T_{bg} of value 560 K. We have solved this equation to estimate the optical depths τ_1 at the lower frequency $v_1 = 330$ MHz towards the components of W43 and inferred their thermal/non-thermal nature; our inferences are listed in the last column of the table.

As seen from Table 1, there is only one thermal component, G30.8 − 0.0, that has an average optical depth exceeding unity at the resolution of 2.6 arcmin. The total flux density of G30.8 − 0.0 has been measured to be 86.5 Jy at 5 GHz (Goss & Shaver 1970) and 82 Jy at 10.6 GHz (MacLeod & Doherty 1968); the spectrum of this source in the range 5–10 GHz appears consistent with that expected towards optically thin H II regions. The flux density of G30.8 − 0.0, as measured by integrating the emission from this object in Fig. 1, is 60 Jy and this value is comparable to

Table 1. Sources in the W43 field.

Source name	RA (J2000.0)	DEC (J2000.0)	Peak flux density S_1 (330 MHz)	Peak flux density S_2 (5 GHz)	Comments
G29.94−0.04	18 46 07.5	−02 41 44	3.6	5.2	Thermal, $\tau_1 \approx 1.0$
G30.23−0.14	18 47 00.8	−02 28 19	1.5	1.7	Thermal, $\tau_1 \approx 0.4$
G30.40−0.24	18 47 40.3	−02 21 14	1.4	1.8	Thermal, $\tau_1 \approx 0.5$
G30.47−0.04	18 47 03.1	−02 12 33	0.86	1.2	Thermal, $\tau_1 \approx 0.4$
G30.50−0.29	18 48 02.6	−02 17 38	0.86	1.1	Thermal, $\tau_1 \approx 0.3$
G30.51−0.45	18 48 39.1	−02 20 42	0.77	0.8	Thermal, $\tau_1 \approx 0.2$
G30.54+0.02	18 47 00.1	−02 06 37	0.95	1.9	Thermal, $\tau_1 \approx 0.9$
G30.61−0.75	18 49 51.1	−02 25 14	0.64	—	Non-thermal
G30.69−0.26	18 48 17.0	−02 06 30	1.8	2.4	Thermal, $\tau_1 \approx 0.6$
G30.70−0.63	18 49 36.1	−02 16 31	1.6	0.3	Non-thermal
G30.78−0.03	18 47 38.6	−02 56 17	8.1	27	Thermal, $\tau_1 \approx 3.7$
G30.85+0.13	18 47 09.2	−01 47 16	1.3	1.9	Thermal, $\tau_1 \approx 0.6$
G31.00−0.30	18 48 58.1	−01 51 31	0.93	0.4	Non-thermal
G31.05+0.48	18 46 17.1	−01 26 56	0.89	1.0	Thermal, $\tau_1 \approx 0.3$
G31.05+0.08	18 47 43.2	−01 38 00	1.8	1.9	Thermal, $\tau_1 \approx 0.3$
G31.13+0.28	18 47 09.4	−01 28 31	0.76	0.9	Thermal, $\tau_1 \approx 0.3$
G31.38−0.38	18 49 59.2	−01 32 49	5.0	0.5	Non-thermal
G31.40−0.26	18 49 34.4	−01 28 30	1.1	1.3	Thermal, $\tau_1 \approx 0.3$

the value of 63 Jy estimated to be the flux density at 408 MHz (Shaver 1969). The spectrum has clearly turned over between 0.4 and 5 GHz; however, the average opacity over the region is only about 1.4 at 330 MHz. The comparison in Table 1 indicates that the opacity at 330 MHz towards the peak of G30.8 − 0.0 exceeds 3.7 at resolutions $\lesssim 2.6$ arcmin. Comparing the 330-MHz image with the 408-MHz image in Shaver (1969), we find that the ratio of peak intensities, S_{330}/S_{408}, is 0.8 as compared with the value of ≈ 0.6 that would be expected if the H II region were isothermal and opaque along the line of sight.

An arc-like feature, with an angular extent of about 70 arcmin (corresponding to a linear extent of 160 pc if the feature is at the distance of the W43 complex), is seen to run across the W43 complex in a roughly north-west to south-easterly direction (Fig. 1). This feature is also noticeable in earlier images of the large-scale radio structure of W43 (for example, Goss & Shaver 1970). The arc may be a super-bubble blown by an association of massive stars in the complex or it could be a result of a supernova of long ago.

4 330-MHz IMAGE OF M17

The 330-MHz image of M17 (also known by the names Omega nebula, NGC 6618, W38 or S45), made with a beam of 77.3×60.7 arcsec^2 FWHM at a position angle of $24°6$, is shown in Fig. 2. The photometric distance to M17 has been estimated to be 2.2 kpc (Chini, Elsässer & Neckel 1980) and this is in agreement with the kinematic distance (Reifenstein et al. 1970); the distance estimate implies that 10 arcmin in Fig. 2 corresponds to a linear size of 6.4 pc. The peak flux density towards M17 is 2.91 Jy beam^{-1}.

The 408-MHz all-sky survey (Haslam et al. 1982) has a peak brightness temperature ≈ 600 K towards M17, and the mean brightness of the sky surrounding the source appears to be 480–500 K. Since the flux density of M17 is itself expected to contribute about 200 K within the survey beam, we estimate the uniform Galactic background towards M17 to be in the range 400–500 K. The 408-MHz image of the Galactic plane presented by Large et al. (1961) also indicates a value of 450 ± 50 K for the background temperature
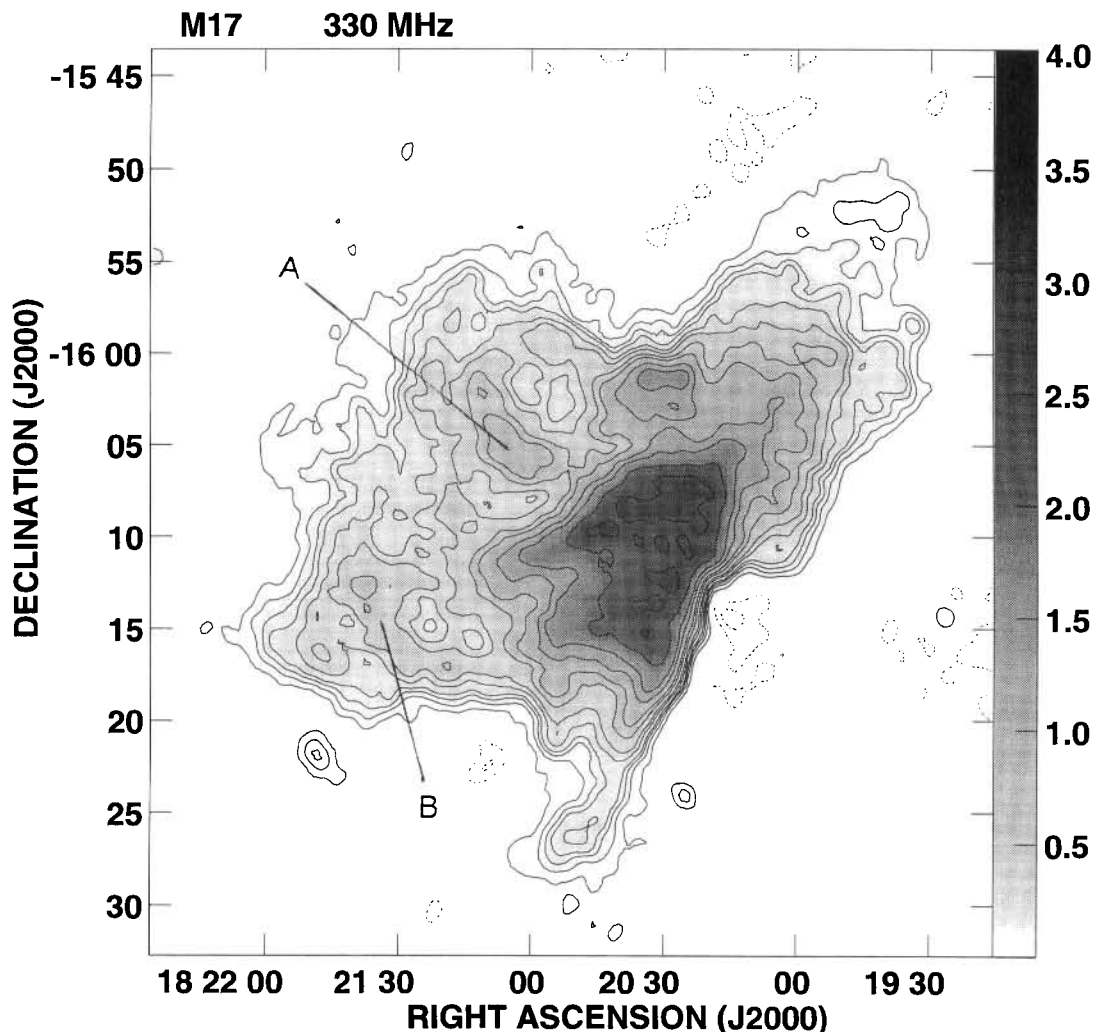

Figure 2. 330-MHz image of M17 made with a beam of 77.3×60.7 arcsec^2 at a PA of $24°6$. Contours are at 10 mJy beam$^{-1} \times (-8, -4, 4, 8, 12, 16, 24, 32, 48, 64, 96, 128, 192, 256)$. Grey-scales are shown in the range 0–4 Jy beam^{-1}. Two shell-like structures are marked A and B.

towards M17. As was the case for W43, the image of M17 has been made with the VLA and consequently the uniform Galactic synchrotron emission present in the sky towards M17 will be missing in the synthetic image. We may conclude that the uniform temperature missing in our 330-MHz interferometric image is 800 ± 100 K. In the image with the beam of 77.3×60.7 arcsec^2 FWHM, the missing uniform flux density is 0.3 Jy beam^{-1}.

Astrophysical data on M17 available up to 1975 have been compiled by Goudis (1976). The radio continuum spectrum of the nebula is summarized over the range 0.086 to 100 GHz and suggests thermal bremsstrahlung emission with a low-frequency turn-over at about 1 GHz owing to self-absorption. The total flux density of M17 at 330 MHz, as obtained by integrating the intensity over the entire source in Fig. 2, is 277 Jy. This estimate of the flux density of M17 at 330 MHz exceeds the value of 165 Jy suggested by the radio spectrum compiled in Goudis (1976): the VLA 330-MHz observations have probably imaged more of the extended emission associated with M17 as compared with the earlier low-frequency observations. However, if we restrict the integration to the region containing G15.1 − 0.7 and G15.0 − 0.7, we obtain a flux density of ≈ 170 Jy. Shaver (1969) estimates the flux density of M17 to be ≈ 275 Jy at 408 MHz and his image primarily covers the regions G15.1 − 0.7 and G15.0 − 0.7; this region, therefore, is inferred to have a spectral index $\alpha \gtrsim 2$ beween 330 and 408 MHz implying that the region appears to be a blackbody radiator at these frequencies. The estimate of < 10 Jy for the flux density at 86 MHz (Mills, Little & Sheridan 1956) implies a spectral index $\alpha > 2.5$ between 330 and 86 MHz. An isothermal H ii region is expected to have $\alpha \leq 2$; the index takes the value 2 when the region is opaque, then the observed brightness temperature is the physical electron temperature T_e at roughly the location at which the optical depth along the line of sight reaches unity. Opacity decreases with increasing frequency and consequently we may expect the observed brightness temperature at higher frequencies to be a measure of the T_e in regions located further within the nebula along the line of sight. If the electron temperature in an opaque H ii region decreases radially away from its centre, the observed brightness temperature may be expected to increase with observing frequency, and the spectral index α may exceed 2. Therefore, the low-frequency spectral index of M17 indicates the existence of lower temperature thermal gas along the line of sight to and, perhaps, surrounding M17.

In the optically thin regime of the radio continuum spectrum, the entire M17 nebulosity has been imaged at 4.875 GHz with a resolution of 2.6 arcmin (Altenhoff et al. 1978). A comparison shows that the VLA 330-MHz image reproduces extended structure up to 0.6–0.7° scale, whereas the radio nebulosity around M17, that is probably associated with it, extends to a maximum scale of 0.7–0.8°. There could be some missing flux density in the 330-MHz image corresponding to at most 0.1 Jy in beams of FWHM 77.3×60.7 arcsec^2.

With a 2-arcmin FWHM beam, M17 has been imaged at 15.4 GHz (Schraml & Mezger 1969) and the brightest region has been resolved into the two components: G15.1 − 0.7 and G15.0 − 0.7. It may be noted here that images of these components with resolutions of 0.85 arcmin

at 1.4 GHz (Löbert & Goss 1978) and 0.75 arcmin at 43.3 GHz (Akabane et al. 1989) have shown the components to have bar-like morphologies and resolved the northern bar, G15.1 − 0.7, into three components. An arcsec-resolution VLA study of M17 (Felli, Churchwell & Massi 1984) has revealed small-scale clumping throughout these bars. The continuum intensity in the 330-MHz image of M17 appears saturated over the entire region covering G15.1 − 0.7 and G15.0 − 0.7. This is consistent with the above-mentioned finding, based on the spectral index, that the region should appear to be a blackbody radiator at this frequency. Convolving the 330-MHz image to the 2-arcmin FWHM resolution of the 15.4-GHz image, we find that the flux density ratio $S_{15.4}/S_{0.33}$ is 9.5 and 6.3 towards G15.0 − 0.7 and G15.1 − 0.7, respectively. Assuming isothermal gaseous nebulae and following the prescription outlined in the preceeding section, we infer that the optical depths towards the southern and northern bars are 12 and 8 respectively at 330 MHz. Although the intensity at 15.4 GHz, and consequently the EM, is higher towards G15.0 − 0.7 as compared with that towards G15.1 − 0.7, the 330-MHz intensity is higher towards G15.1 + 0.7: the opacity at 330-MHz is higher towards the southern bar and this is probably owing to both lower electron temperatures as well as higher EM.

The ratio continuum spectrum of M17 shows a low-frequency turn-over at ≈ 1 GHz and below this frequency the nebula has been imaged at 408 MHz with a resolution of 3 arcmin (Shaver 1969). We have smoothed the 330-MHz image to the resolution of the 408-MHz image and added a uniform flux density of 2.2 Jy beam^{-1}, corresponding to the Galactic background that is missed in the 330-MHz interferometric image. The spectral index towards the peaks of G15.0 − 0.7 and G15.1 − 0.7 were then computed to be 2.3 and 2.2 respectively between 330 and 408 MHz; similar to the value obtained above based on the total flux densities in these components. Once again, the spectral indices are marginally steeper than that expected towards isothermal opaque H ii regions and indicative of relatively cooler plasma along the line of sight to M17.

Shell-like structures appear at the positions marked A and B in Fig. 2. The A shell is almost complete, but in the case of B only a sector is seen. The Hα contour image of M17 (Ishida & Kawajiri 1968) shows an arc-like structure corresponding to shell B and an emission maximum at the brightest part of shell A. It may be noted that such arc-like, possibly thermal, features were also observed in the W51 complex (Subrahmanyan & Goss 1995). These shells have a typical scale of 10 pc and are perhaps thermal emission from parts of bubbles created by the interaction of winds from massive stars and the interstellar medium (see, for example, McCray 1983 for a review).

5   ELECTRON TEMPERATURES TOWARDS G30.8 − 0.0, G15.0 − 0.7 AND G15.1 − 0.7

The brightness temperature observed in an interferometric image towards an opaque H ii region, corrected for the finite resolution of the image, the optical depth along the line of sight, and for the uniform background that may be missing, yields an estimate of the electron temperature towards the H ii region (see, for example, Subrahmanyan & Goss 1995). Estimates of the electron temperature (T_e)

based on radio continuum images are independent of assumptions regarding departures from local thermodynamic equilibrium (LTE) conditions. Most estimates derived from radio recombination lines, however, assume LTE and consequently derive what is commonly referred to as the LTE electron temperature (T_e^*).

G30.8 − 0.0, with an EM = 7×10^5 (Downes et al. 1980), is the highest EM H II region in W43. The peak flux density of 2.02 Jy beam^{-1} observed towards G30.8 − 0.0 in Fig. 1 corresponds to a brightness temperature of 4600 K. We have convolved the image to progressively poorer resolutions and examined the decrease in the beam-averaged brightness with image resolution. These data are poorly fitted if the source is modelled as an opaque disk; however, a Gaussian model with FWHM of 270 arcsec and peak brightness of 4900 K fits the data. We estimate the deconvolved peak brightness towards G30.8 − 0.0 to be in the range 4600–4900 K. The optical depth towards the emission peak exceeds 3.7, implying a correction factor in the range 1.00–1.03 for converting the observed brightness to electron temperature. We also add a value of 560 ± 50 K to account for the missing background brightness in the W43 image and finally arrive at an estimate of 5410 ± 300 K for the electron temperature in G30.8 − 0.0.

Schraml & Mezger (1969), as also Wilson et al. (1970), estimate the LTE electron temperature $T_e^* = 5640$ K towards G30.8 − 0.0 from their H109α recombination line observations. Downes et al. (1980) estimate LTE electron temperature $T_e^* = 6000 \pm 1000$ K from their H110α survey. From his 408-MHz continuum image, Shaver (1969) estimates $T_e = 5900 \pm 600$ K. All these estimates for T_e in G30.8 − 0.0 are consistent with the value we derive above at 330 MHz.

The peak intensities in the 330-MHz image (Fig. 2) towards G15.0 − 0.7 and G15.1 − 0.7 and 2.75 and 2.91 Jy beam^{-1} respectively; the corresponding beam-averaged brightness temperatures are 6690 and 7080 K. As discussed above in the case of W43, we have again convolved the image in Fig. 2 to progressively poorer resolutions to derive the decrease in beam-averaged brightness with resolution. If we model the sources as having Gaussian profiles, we infer that their peak brightness temperatures do not exceed 7400 and 7550 K respectively for G15.0 − 0.7 and G15.1 − 0.7. However, if we model the sources as opaque discs, as may be expected because the optical depths towards these directions exceed 8–12, we infer that the disc brightness temperatures cannot exceed 6800 and 7200 K respectively for G15.0 − 0.7 and G15.1 − 0.7. The correction factor of $(1 - e^{-\tau})^{-1}$ for the finite optical depth towards these regions is less than 0.01 per cent because the optical depths exceed eight. To these corrections we add 800 ± 100 K for the missing uniform background. We conclude that the electron temperatures towards G15.0 − 0.7 and G15.1 − 0.7 are within the ranges 7390–8300 K and 7780–8450 K respectively; the likely values are 7600 and 8000 K.

Downes et al. (1980) derived the LTE electron temperature towards M17 to be 9100 ± 1000 K from their observations of the H110α transition. Hjellming & Gordon (1971) derive a non-LTE solution for T_e by combining α transitions with higher-order recombination lines: they estimate

$T_e = 7500 \pm 850$ K. Based on the 408-MHz continuum image of M17, Shaver (1969) estimates T_e to be 7850 ± 500 and 8400 ± 500 K respectively towards G15.0 − 0.7 and G15.1 − 0.7. These previous estimates are consistent with the T_e estimate derived above from the 330-MHz observations.

REFERENCES

Akabane K., Sofue Y., Hirabayashi H., Inoue M., 1989, PASJ, 41, 809

Altenhoff W. J., Downes D., Pauls T., Schraml J., 1978, A&AS, 35, 23

Baars J. W. M., Genzel R., Pauliny-Toth I. I. K., Witzel A., 1977, A&A, 61, 99

Chini R., Elsässer H., Neckel Th., 1980, A&A, 91, 186

Copetti M. V. F., Schmidt A. A., 1991, MNRAS, 250, 127

Downes D., Wilson T. L., Bieging J., Wink J., 1980, A&AS, 40, 379

Felli M., Churchwell E., Massi M., 1984, A&A, 136, 53

Gardner F. F., Thomasson P., 1975, A&A, 45, 1

Goss W. M., Shaver P. A., 1970, Aust. J. Phys. Astrophys. Suppl., 14, 1

Goudis C., 1976, Ap. Sp. Sci., 39, 273

Haslam C G. T., Salter C. J., Stoffel H., Wilson W. E., 1982, A&AS, 47, 1

Hjellming R. M., Gordon M. A., 1971, ApJ, 164, 47

Ishida K., Kawajiri N., 1968, PASJ, 20, 95

Large M. I., Mathewson D. S., Haslam C. G. T., 1961, MNRAS, 123, 112

Lester D. F., Dinerstein H. L., Werner M. W., Harvey P. M., Evans II N. J., Brown R. L., 1985, ApJ, 296, 565

Liszt H. S., Braun R., Greisen E. W., 1993, AJ, 106, 2349

Löbert W., Goss W. M., 1978, MNRAS, 183, 119

MacLeod J. M., Doherty L. H., 1968, ApJ, 154, 833

McCray R., 1983, in West R. M., ed., Highlights of Astronomy Vol. 6. Reidel, Dordrecht, p. 565

Mills B. Y., Little A. G., Sheridan K. V., 1956, Aust. J. Phys., 9, 218

Napier P. J., Thompson A. R., Ekers R. D., 1983, Proc. IEEE, 71, 1295

Osterbrock D. E., 1989, Astrophysics of Gaseous Nebulae and Active Galactic Nuclei. University Science Books, Mill Valley, CA

Perley R., Crane P., 1986, NRAO Newsl., 27, 9

Reifenstein III E. C., Wilson T. L., Burke B. F., Mezger P. G., Altenhoff W. J., 1970, A&A, 4, 357

Schraml J., Mezger P. G., 1969, ApJ, 156, 269

Shaver P. A., 1969, MNRAS, 142, 273

Shaver P. A., Goss W. M., 1970, Aust. J. Phys. Astrophys. Suppl., 14, 77

Subrahmanyan R., 1992a, MNRAS, 254, 291

Subrahmanyan R., 1992b, MNRAS, 254, 719

Subrahmanyan R., Goss W. M., 1995, MNRAS, 275, 755

Wilson T. L., Mezger P. G., Gardner F. F., Milne D. K., 1970, A&A, 6, 364